

Next Generation GPS Ground Control Segment (OCX) Navigation Design

Willy Bertiger¹, Yoaz Bar-Sever¹, Nate Harvey¹, Kevin Miller¹, Larry Romans¹, Jan Weiss¹

Larry Doyle², Tara Solorzano², John Petzinger²

Al Stell³

¹*Jet Propulsion Laboratory, California Institute of Technology, Pasadena, California, USA*

²*ITT*

³*Raytheon*

Biographies

Willy Bertiger received his Ph.D. in Mathematics from the University of California, Berkeley, in 1976. In 1985, he began work at JPL as a Member of the Technical Staff in the Earth Orbiter Systems Group. His work at JPL has been focused on the use of GPS, including high precision orbit determination, positioning, geodesy, remote sensing, and wide area differential systems.

Abstract

In February 2010, a Raytheon-led team was selected by The Air Force to develop, implement, and operate the next generation GPS ground control segment (OCX). To meet and exceed the demanding OCX navigation performance requirements, the Raytheon team partnered with ITT (Navigation lead) and JPL to adapt major elements of JPL's navigation technology, proven in the operations of the Global Differential GPS (GDGPS) System. Key design goals for the navigation subsystem include accurate ephemeris and clock accuracy (user range error), ease of model upgrades, and a smooth and safe transition from the legacy system to OCX.

We will describe key elements of the innovative architecture of the OCX navigation subsystem, and demonstrate the anticipated performance of the system through high fidelity simulations with actual GPS measurements.

Introduction

The Global Positioning System (GPS) has evolved since its inception through several generations of satellites and many minor and major improvements to its control segment (CS). In recent years it has been delivering a broadcast user range error (URE) that is consistently better than 1 m. The most recent evolution is embodied in the Air Force's competitive procurement of the Next Generation Operational Control Segment, called OCX. OCX includes a complete modernization of the CS, including new architecture, infrastructure, hardware, and software required to comply with a set of demanding performance requirements. In February 2010, the OCX development and implementation contract was awarded to an industry team, lead by Raytheon.

Within the Raytheon team ITT (as lead) and JPL have the responsibility for the Navigation System, encompassing the positioning, navigation, and timing capabilities of GPS. At the core of the Navigation System is the orbit determination and ephemeris prediction software. In this article we describe our approach for complying with the navigation requirements, the supporting analysis, and the key architectural elements of the navigation system.

Key OCX Performance Requirements

User Range Error (URE)

Because the error in pseudorange-based kinematic positioning is, to first order, directly proportional to the URE (via the Dilution of Precision - DOP factor [Jorgensen, 1984]), URE is a key quality metric for the GPS signal. It is a function of both the error in the broadcast satellite ephemeris and the broadcast satellite clock. In the OCX requirements, URE is defined as:

$$URE = \sqrt{(dr - dt)^2 + (dc^2 + di^2)} / 50 \quad (1)$$

where dr is the error in the satellite's radial position, dt is the error in the satellites clock, dc is the error in cross-track position, and di is the error in-track position. Table 1 summarizes the OCX URE requirements as a function of Age of Data (AOD). AOD is the lag between the epoch time of the orbit and clock values and the time tag of the last measurements used in the orbit and clock estimation. The specifications can be broadly separated into legacy satellites (GPS II) and GPS III satellites since the broadcast message formats have different levels of precision/fit errors. We ignore here slight differences in specification for the different signals, such as M-code and P-code. A portion of the URE budget is allocated to the Space Segment (SS), for example, to account for the unpredictable stochastic nature of the Space Vehicle (SV) clocks. The column labeled "Overall" is the error a user would see, including contribution from the SS and the CS.

Table 1, OCX URE requirements

	Legacy P(Y),CA		GPS III	
Age of Data	URE RMS (meters)		URE RMS (meters)	
	Overall	CS	Overall	CS
0 hours	0.30	0.30	0.15	0.15
1 hour	0.35	0.30	0.25	0.16
24 hours	1.50	0.70	1.50	0.65
14 days	50	20	50	20

It is interesting to compare the OCX performance requirements for the URE with the actual present and historical performance of GPS. The GPS signal in space URE has been measured in real-time by the GDGPS System since 2003 under contract with the Air Force.. Figure 1, shows

the RMS of all the 30 second points within a day together with a smooth curve fit to those points. Since the Block IIA satellites perform differently than the Block IIR satellites, we have separated the statistics into these two SV types. The plot demonstrates the significant improvements to the GPS system over the last seven years during which the URE for the IIR satellites changed from about 90 cm to 50 cm RMS. Errors in the GDGPS URE are about 9 cm.

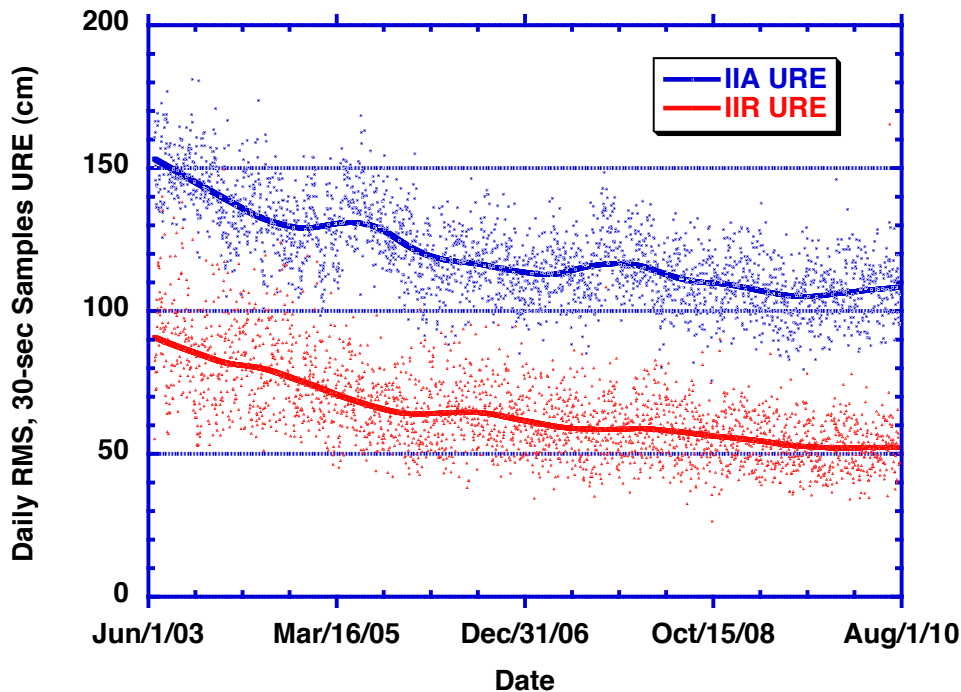


Figure 1, RMS 30-second sampled GPS broadcast URE over each day, June 2003 through July 2010, as measured in real time by the GDGPS System. Solid lines are smooth curves drawn through the daily RMS values.

We cannot directly compare this measure of the current and past performance with Table 1, since the age of data (AOD) over a day in the broadcast message varies. The Block IIR actual performance is certainly close to the OCX requirements.

Design Heritage and Operational Experience with the GDGPS System

The OCX orbit determination and ephemeris prediction software is based on JPL's Real Time GIPSY (RTG) software, operationally proven within the Global Differential (GDGPS) System, which is functionally very similar to the current GPS Operational Control Segment (OCS) navigation system.

The GDGPS System is a GPS augmentation system on a global scale. The fundamental tenet of this architecture is a *state-space* approach, where the orbits of the GPS satellites are precisely modeled, and the primary estimated parameters are the satellite epoch states and instantaneous clock offset. The clock offsets are estimated as white noise process every epoch. This approach guarantees that the estimated ephemerides are globally and uniformly valid. A commercial North American Wide Area Differential GPS (WADGPS) system based on the JPL architecture and software was first implemented in 1995 by SATLOC Inc., primarily for the agricultural market

[Bertiger et al., 1998]. In 1996 the Federal Aviation Administration (FAA) selected the JPL architecture and software for their prototype Wide Area Augmentation System (WAAS). The system has been implemented and operated by Raytheon, the prime WAAS contractor.

The GDGPS ground network of real time GPS receivers consists of more than 100 semi-codeless dual frequency receivers, of which the large majority have been installed, operated, and maintained by JPL, and the rest are contributed by a number of commercial, and institutional partners (Figure 2). Redundancy is the key to the system's reliability, by ensuring that there are no single points of failure in the system. GPS measurements collected at the 20-fold redundant tracking network (at anytime each SV is tracked by an average of 20 stations) are streamed in parallel to three geographically-separated Operations Centers. Data processing is carried at the Operations Centers on redundant chains of computers using the RTG software package, which estimates the GPS orbit and clock states in real time, and derives a host of by-products. Two (redundant) United States Naval Observatory (USNO) Master Clock sites provide reference time for the GDGPS System (The USNO Master Clock also provides the official Universal Time Coordinated (UTC) reference for the U.S. Department of Defense).

GDGPS has been operational since 2000. A complete array of real-time GPS state information, environmental data, and ancillary products are available in support of the most demanding GPS Augmentation operations, Assisted GPS (A-GPS) services, situational assessment, and environmental monitoring - globally, uniformly, accurately, and reliably [www.gdgps.net].

The quality of the GDGPS real-time and predicted GPS ephemerides and clocks, has been verified against the cm-level accurate JPL and IGS post-processed orbit and clock products. Typical accuracies in terms of URE are summarized in Table 2

Table 2. URE for key GDGPS products, measured against JPL post-processed orbit and clock products

Age of Data	Median URE
0 Hours	0.09 m
24 Hours	0.5 m
7 Days	8.4 m

Using an appropriate subset of its tracking network, GDGPS is ideally suited to serve as a test bed and validation tool for the high performance OCX navigation software, significantly reducing Program risk by enabling test and validation with real data, in a real-time operational environment.



Figure 2. The network of real-time GPS tracking sites feeding the GDGPS System as of August 2010

Performance Analysis

In our studies of the OCX orbit determination performance, we have strived to use actual GPS data instead of simulation wherever possible to account for the many errors that are difficult to simulate. However, one error source that maybe significantly different in future GPS satellites is the space vehicle clock, since the formal stability specification is more conservative than the actual on-orbit performance of today's IIR clocks. For this error source, we use a combination of real data and simulated clock behavior.

We use the IGS Final Combined orbit and clock products as 'truth' [http://igsb.jpl.nasa.gov/components/prods_cb.html]. These products are a combination of IGS analysis center contributions, including JPL's. The agreement between the contributed solutions and the Combined solution is typically at the few cm level. Inter-comparisons with independent satellite laser-ranging measurements carried out routinely at JPL and elsewhere confirm an orbit quality assessment of better than 5 cm RMS in the radial coordinate [eg, Urschl et al., "Validation of GNSS orbits using SLR observations", *Advances in Space Research* 36. 2005].

Monitor Station Distribution/Selection

The number and distribution of the tracking network is a key factor in zero age of data (0AOD) URE performance. With sufficient number of monitor stations it is possible to estimate all system clock (satellites and monitor station) as white noise. This is the approach employed by the GDGPS System because it is insensitive to clock anomalies, which are not uncommon. To analyze the impact of tracking network size on orbit determination accuracy we selected several well-distributed stations. Figure 3, depicts the resulting radial error, which along with the clock is the dominant term in the URE value as a function of the number of monitor stations. The knee in the curve, or the point of diminishing returns occurs approximately with 15-17 monitor sites.

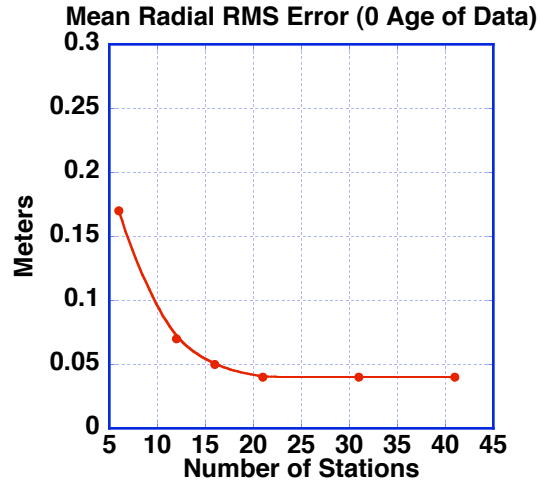


Figure 3. RMS Radial orbit error as a function of monitor network size. Analysis performed using a filter only orbit estimation scheme.

The present set of 17 well-distributed OCS monitor stations, consisting of six US Air Force stations and 11 National Geospatial-Intelligence Agency (NGA) stations, was therefore selected as the baseline monitor station network for OCX. In Fig. 4, we show the locations of these government operated stations along with International GNSS Service (IGS) stations at nearby locations used in the 16 station data point, Fig. 3. There were a couple of Government locations which did not have close matches with publicly available data that met our minimum data quality checks. The Government locations are arguably slightly better for a uniform distribution over the Earth.

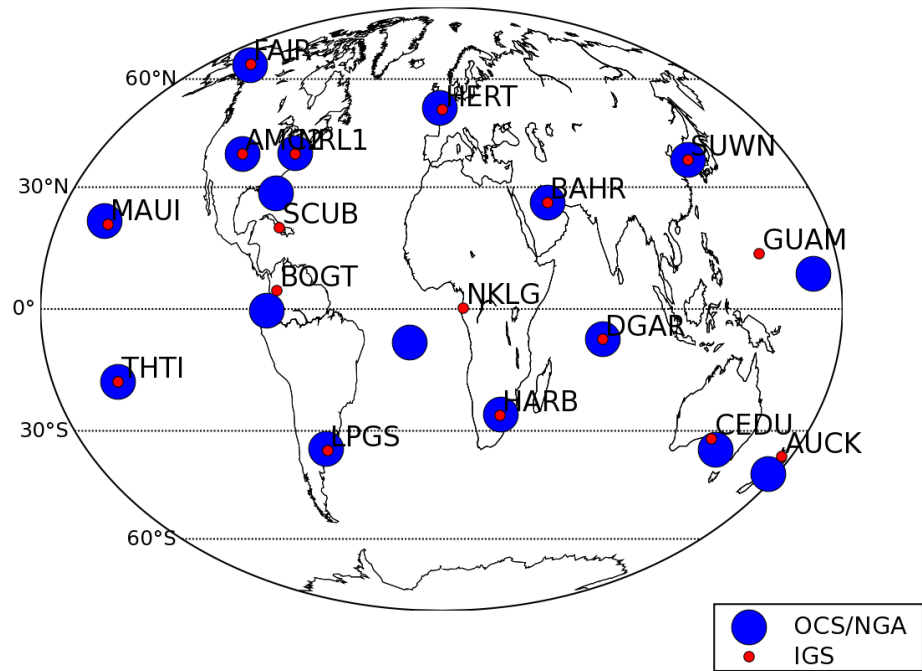


Figure 4, IGS stations used in place of 17 OCS monitor stations.

Data Processing Software and Configuration

To emulate our proposed OCX Kalman Filter navigation software, we used the JPL’s GIPSY software set [Webb & Zumberge, “An introduction to GIPSY-OASIS II”, JPL Publication D11088, 1997]. We ran this software in a **forward-filter-only** mode, which will produce the same results as a forward running filter executing in real-time. We chose GIPSY instead of its real time version, RTG, because it has more powerful input/output options that are more convenient for this kind of analysis. Table 3, lists the adjusted filter states and their stochastic properties. Since we wanted to sample data over 24 hours, we ran the GIPSY filter through 3-days of data and then used the last day to compute statistics. By the 3rd day the filter has settled to steady state. The filter processes phase and pseudorange data with a relative weight of 100:1 in favor of the phase data. Although phase data are biased relative to pseudorange, the data have much smaller random errors and much small multi-path errors.

Table: 3, Kalman Filter States and their characteristics

Parameter	Type	Apriori Sigma	Process Noise	Update Interval (Seconds)	Time Correlation

Satellite Position/Velocity	Constant/Epoch State	10 meters, 1 cm/sec			
Solar Scale	Constant	0.1			
Y-Bias	Constant	0.1			
Once Per Rev Along Track and Cross Track Acceleration	Stochastic	1 nm/sec ²	1 nm/sec ² /sec ^{0.5}	43201	Random Walk
Wet Troposphere Zenith Delay	Stochastic	50 cm	5x10 ⁻³ cm/sec ^{0.5}	300	Random Walk
Gradient Troposphere	Stochastic	100 cm	5x10 ⁻⁴ cm/sec ^{0.5}	300	Random Walk
Station and SV Clocks	Stochastic	0.1 secs	0.1 secs	300	White Noise

White Noise Clock Estimates

Notice that in our proposed filter for OCX, we are treating the satellite clocks as white noise. This is different from the current ground segment processing (OCS) which models the clocks as a quadratic function of time with some process noise on the quadratic coefficients determined by the long-term clock behavior characterized by the Hadamard deviation. Indeed, constraining the clock model was necessary when the tracking network was limited to 5 stations. However, this is not necessary with a well-distributed 17-site tracking network. The white noise approach is completely insensitive to the clock time history, and allows detection of clock anomalies such as jumps in frequency.

We have performed extensive analysis to demonstrate the ability of our filter to retrieve actual clock offsets which are independent of the actual clock characteristics. In these tests, we adjust the real data with simulated clock changes for both stations and satellites. The RMS difference between the simulated SV clock and the recovered 0AOD clock was below 0.01 mm for all satellites. We also compared the SV positions for the case with the unmodified data, with the simulated clocks case. The maximum RMS difference over all the satellites on the 3rd day was 1.2 mm in cross-track. The maximum RMS radial and along-track differences were 0.6 and 1.0 mm.

0AOD URE with 17-stations

We processed one month of GPS data spanning, 2008-05-15 to 2008-06-15. For each 24 hour period in our test data set, which was the final day of the 3 day filter-only run, we computed the URE given in the formula above where dr , dt , di , and dc are determined by differencing the filter output every 15 minutes with a truth determined by the IGS Final Combined solution, and also with the JPL Final solution. A small percentage of the 15-minute epochs are not used due to large formal errors on the white-noise clock estimate for the SV or missing data from the truth orbits and clocks. The large formal errors are due to instances of poor observation, either due to deficient geometry or data quality problems, or both. Note that this will have almost no effect on our ability to predict the clock into the future for uploads, since it is the long-term behavior of the clock that dominates prediction error. At each point in time, as discussed above, $dr-dt$, is adjusted by the mean over the entire constellation to remove the effect of an arbitrary reference clock. Figure 5 shows a histogram of 24-hour RMS URE values all SVNs for all days in the study. The average 24-hour URE relative to the IGS in the 865 samples is 6.7 cm. The average relative to the JPL final was 6.5 cm over the 869 samples. A small part of the difference is due to the error in the truth solution. As a bound of the error in the truth, we can use the 24-hour RMS URE obtained from the difference of JPL and IGS. The mean of all these 24-hour RMS values was 2.5 cm with a median of 2.0 cm. Only 1.8% of the 24-hour URE values relative to the IGS 'truth' are greater than 15 cm (16 out of 869).

Our analysis shows that the URE is dominated by the clock error, with mean daily RMS clock error of 7.1 cm. The radial orbit error is nearly insignificant with a mean daily RMS radial error of 3.7 cm.

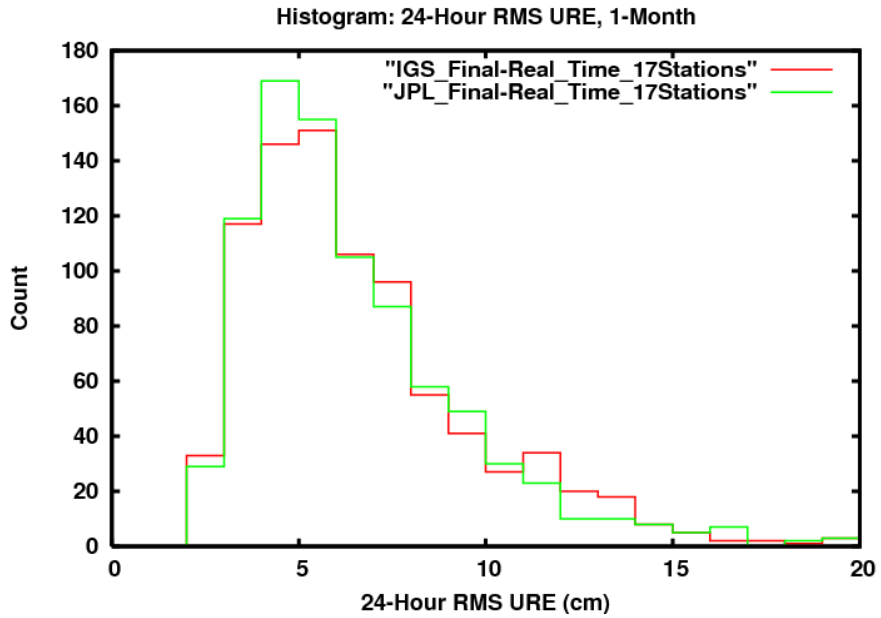


Figure 5. Histogram of 24-hour UREs, RMS URE is computed using both IGS Final Orbits/Clocks (865 24-Hour RMS values) and JPL Final Orbits/Clocks as truth (869 24-Hour RMS values)

Finally, in Figure 6 we compute the 24-Hour RMS URE over all the satellites in the constellation for each day in the month of data. The values are fairly uniform in time with a maximum of about 8 cm.

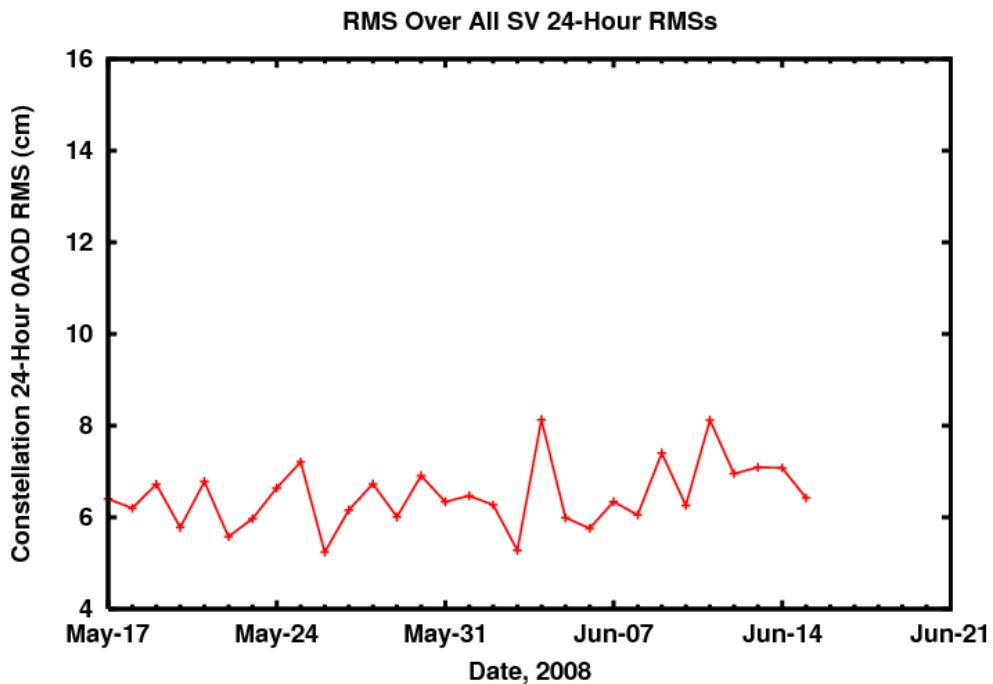


Figure 6. 24 Hour RMS URE over constellation, May 15 – June 15 2008

URE for Predicted Orbits and Clocks

Table 1, above, summarizes the OCX requirements for predictions of 1 hour, 24 hours, and 14 days. For predictions longer than 1 hour, the stability of the space clock is the dominant error source, dominating the measurement/estimation errors. The contribution of the SV clock frequency stability to the total error budget of predicted URE is currently allocated to the Space Segment. Responsibility for force models is divided between the SS and CS, but we will focus here on the overall error and gloss over the allocations. For the force models, regardless of allocation, we assume that the models will be no worse than the Block IIR satellites currently in orbit which are distinctly better than the Block IIA spacecraft. Here again we will try to use real data for our error analysis, but since the clock dominates the error for long-term prediction and the specified clocks are not as good as some of the IIR clocks in orbit, we will simulate the effects of the stochastic clock errors.

Per the OCX specification, the maximum Hadamard deviation for the spacecraft clock must fall below a piecewise linear function on a log-log plot defined by the three points in Table 4.

Table 4, Maximum allowed Hadamard Deviation for the space clocks is piecewise linear on a log-log passing through the 3 points.

Averaging Time (Tau)	Hadamard Deviation
1 sec.	7e-12
54,444 sec. (about 15 hours)	3e-14
1,209,600 sec. (14 days)	3e-14

To account for measurement errors, we used the procedure discussed above where we substituted simulated clock values with a close approximation to the required clocks for the recovered clock values in the real data.

Orbit Prediction

Following the approach we presently employ in the GDGPS System, our design for the OCX navigation system calls for carrying the orbit (and clock) prediction in a parallel process to the OOAD orbit determination process. The prediction process uses present and past OOAD states estimates from the orbit determination filter, fits a model to these data, and propagates the model forward. This approach allows independent optimization for different prediction lengths. For GPS orbit prediction, three days of estimated orbital state records (position and velocity) for each satellite are used in a least squares scheme to adjust a parameterized model of the satellite dynamics. The key adjustable model parameters are typically the solar scale, Y-bias, and a set of parameters representing empirical constant and cyclic accelerations. However, the estimated model parameters may be different for different satellite types and for different orbital regimes (in particular eclipse season). Note the models used here for prediction maybe different from those of the OOAD filter and may also be different from the state vector propagation used on-board the space vehicle. The fit process takes a few seconds and adds insignificantly to the

latency of any OCX upload process. The data interface to the space vehicle is a state vector; we show in a later section that the model for propagating the state vector does not need to be identical to meet the system accuracy requirements. Allowing these models to vary, allows for evolving the models used in the ground segment both in the 0AOD filter and in the prediction process.

We generated predictions once per day, for each of the 30 days in our 0AOD test from May 5 through June 5 2008. Since this is real GPS data, samples that span satellite maneuvers or large gaps in data were removed. The remaining samples constitute a large set of data, which enables us to further classify the performance according to satellite type, and eclipse regime. These predictions are compared to the final post-processed JPL orbits to assess their contribution to the URE. Tables 5 and 6, summarize the results for IIA and IIR satellites. Figure 7, shows the distribution of the IIR URE values for the 24-hour prediction. As might be expected it is not symmetric about the RMS.

Table 5, Block IIR satellite URE due to orbit prediction. The two numbers in parenthesis are number of satellites in the RMS error statistic and the number of data points.

Prediction Length	Not Eclipsing	Eclipsing	Eclipsing and Not Eclipsing
1 hour	0.05 m (10, 524)	0.06 m (8, 422)	0.05 m (18, 946)
24 hours	0.10 m (10, 524)	0.10 m (8, 420)	0.10 m (18, 944)
14 days	3.23 m (10, 506)	5.01 m (8, 414)	4.13 m (18, 920)

Table 6, Block IIA satellite URE due to orbit prediction. The two numbers in parenthesis are number of satellites in the RMS error statistic and the number of data points.

Prediction Length	Not Eclipsing	Eclipsing	Eclipsing and Not Eclipsing
1 hour	0.06 m (5, 250)	0.06 m (8, 344)	0.06 m (13, 594)
24 hours	0.09 m (5, 248)	0.16 m (8, 338)	0.14 m (13, 586)
14 days	3.29 m	24.06 m	17.09 m

	(15, 724)	(16, 710)	(31, 1434)
--	-----------	-----------	------------

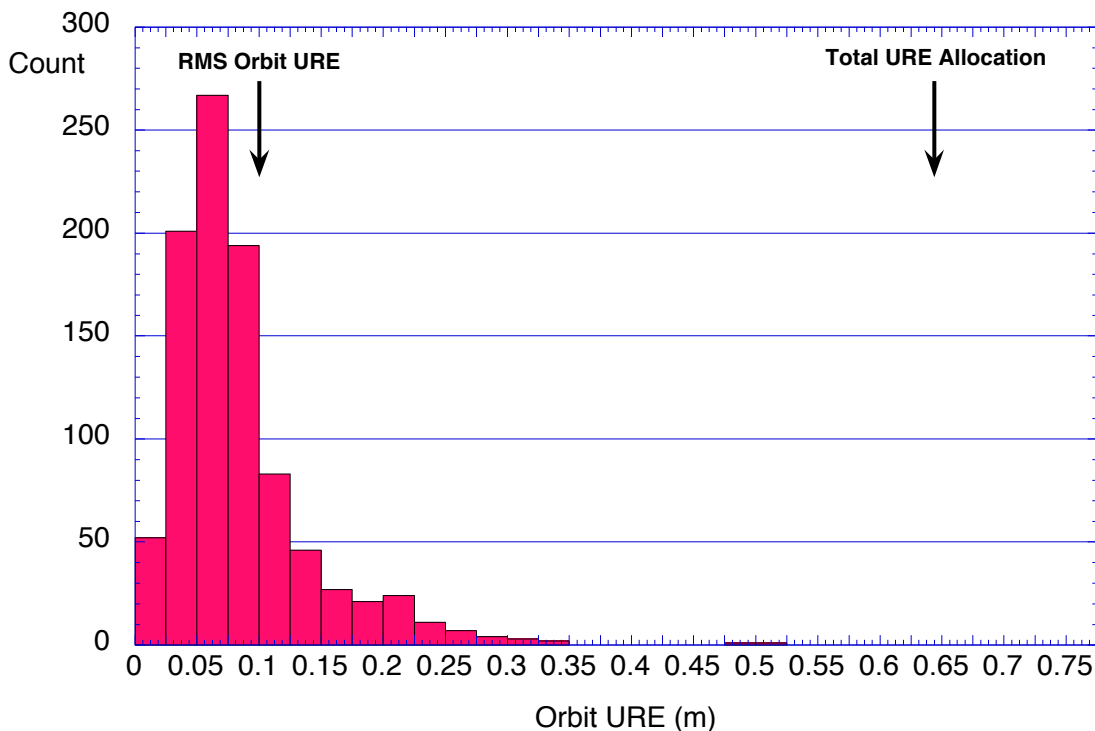


Figure 7, Histogram of orbital URE at 24 hour AOD for all Block IIR satellites (eclipsing and non-eclipsing).

Clock Prediction

In our approach clock prediction, like orbit prediction, is decoupled from the OAOD filter. Here, too, we use a time history of the OAOD recovered clock and a tunable Kalman Filter for Clocks (KFC).

For this analysis we used twenty different simulated satellite clock sequences, each 250 days long, with 1-minute resolution possessing the require Hadamard stability. Reflecting our assumptions about the underlying noise source the sequences include noise contributions from phase random walk, frequency random walk, and frequency flicker noise. The twelve-hour periodic component sometimes found in real clocks were not included, but such a periodic component can be easily removed prior to filtering by comparing long-term average clock behavior at different hours (at the cost of slightly expanded error bars). Real clocks also include jumps in clock behavior, which we can check for (at very little cost to accuracy) by an innovations test, and after finding, expand the covariance matrix until things settle down.

The simulated sequences were decimated to the 1-hour rate (for throughput efficiency), and the first 150 days of each sequence was used to tune the KFC. The remaining portion of the sequence was used to evaluate the predictions. Two types of predictions were carried out:

- 1) Only the simulated clocks were used in the prediction. This is useful to measure the performance of the KFC, and validate its theoretical foundation. We use this approach to assess the contribution to the URE due to “frequency stability”.
- 2) After the KFC was tuned on the first 150 day of each sequence, we added real 0AOD clock errors from our 0AOD URE analysis (difference of our 0AOD clock with the post processed truth solution) to a month-long section of the simulated sequences (the 0AOD URE analysis spanned a full month). The predicted clocks now include real clock measurement errors as well as errors due to the stochastic nature of the clocks, coupled with the KFC clock propagation algorithm. We use this approach to assess the combined effects of measurement error and frequency stability to the URE due to all aspects of clock predictions. The measurement-only contribution can be obtained by subtracting, in quadrature, the URE of the first approach (frequency stability only contributions) from the URE of the second.

The prediction performance for 1 hour, 24 hours, and 14 days were assessed by repeating the prediction in a sliding window manner every hour over a period of one month, thus accumulating a large statistics. Approach #2 (considering measurement errors) was not attempted in the 14 days prediction case because the statistics generated with one month of data would not be large enough. However, the small effect of measurement error as manifested in the 1 hour and 24-hour predictions suggests that the effect of measurements error on 14 day clock prediction is negligible. Table 7, summarizes the errors for the different prediction intervals.

Table 7, URE Errors due to clock prediction error

Age of Data	URE Due Freq. Stability	Total Clock URE (Freq., measurement error)
1 hour	0.12 m (500)	0.14 m (500)
24 hours	1.00 m (477)	1.01 m (477)
14 days	19.14 (2064)	Not Computed

Predicted URE Summary

Adding the total clock errors (just simulated for 14 day clock) and the orbit errors in quadrature, we arrive at the predicted error budget for Block IIR-like satellites shown in Table 8. For 1-hour prediction, with the legacy broadcast there would be a slight additional degradation in performance due to broadcast message fit error.

Table 8, expected predicted URE with Block IIR models and simulated future clocks compared to requirements, modernized signals

Age of Data	Required URE (meters)	Measured URE (meters)
1 hour	0.25	0.15
24 hours	1.50	1.01
14 days	50	19.60

Space Segment Interface via State Vectors

The overall system design defines the transfer of the CS predicted GPS orbit to the space segment via a state vector. The state vector is defined to be the inertial Cartesian coordinate position and velocity at an epoch and some parameters to small force models such as solar pressure. One way to realize the Earth fixed prediction made by the ground segment is for the spacecraft is to have the space segment implement identical models to the ground for the forces on the spacecraft and the transformation between inertial space and Earth fixed coordinates. This has obvious drawbacks for change and maintenance.

To perform the initial tests of this concept, we used a precise representation of the GPS satellites in earth fixed coordinates (ITRF2005) and fit those positions with a force model and Earth Orientation model that were different than those used to produce the time series. RMS differences for an eclipsing satellite over the 24-hour fit period compared to the precise time series were 0.96, 1.82, and 0.74 cm in radial, along-track, and cross-track, respectively. For a non-eclipsing satellite, the differences were 1.10, 1.41, and 0.73 cm. With a 14-day fit, RMS errors for a non-eclipsing satellite were 11.6, 136.8, and 76.0 cm, and 16.6, 31.1, and 42.9 cm for an eclipsing satellite. Note that only the radial errors contribute appreciably to the URE. Neither of these fits was optimized for the time of the broadcast messages.

The Reference Orbit

For the 24-hour AOD study we used the JPL Final GPS orbit solutions (also contributed to the IGS Final Combined solution) as a proxy for an OCX-based propagated ephemeris. It generally agrees with the IGS Final Combined solution at the ~3 cm level. For the 14-day study, we used the IGS Final orbit, which is a weighted combination of the JPL submission and the submissions of other analysis centers. There is some variation in both earth orientation and force modeling among the analysis centers. The orbit is sampled at 15-minute intervals, and expressed in the ITRF2005 earth fixed coordinates in which the orbit was ‘measured’. Our goal is to demonstrate how this ‘truth’ ephemeris can be faithfully and efficiently communicated to a space segment employing a different set of models than used in the generation of the truth ephemeris.

Least Square Orbit Fit

Given an orbit propagation method which can also integrate the variational equations, and an Earth orientation model, the time series expression of the reference orbit can be used in a least squares scheme where a set of epoch state and model parameters are estimated to create a modeled orbit that best fits the time series. We will demonstrate that the force models and Earth

orientation models used in this least squares fit do not have to be identical to the models used in the generation of the reference orbit. Indeed, they only need to be ‘reasonably’ accurate.

Force Model Variation

The JPL Final GPS orbit products are computed using the GSPM04 solar radiation pressure model [Bar-Sever, Y. E., and Kuang, D., *IPN Progress Report 42-160*, JPL, 2004. http://ipnpr.jpl.nasa.gov/progress_report/42-160/title.htm]. To simulate potential differences in force modeling between the space segment and the ground segment we used the simpler T30 model in the least squares fit process [Fliegel, H. F., and T.E. Gallini, “Solar force modeling of Block IIR Global Positioning System satellites”, *Journal of Spacecraft and Rockets*, V 33 No. 6, 1996]. Fig. 8 and Fig. 9 depict the differences in integrating an eclipsing and a non-eclipsing satellite, respectively, using the two solar pressure models (starting from the same epoch state parameters in inertial space). Peak differences for the eclipsing satellite are at the 2-meter level and at the 1.5-meter level for the satellite in full sun. Figure 10 shows the divergence of the two models out to 14 days reaching a maximum difference of about 90 meters.

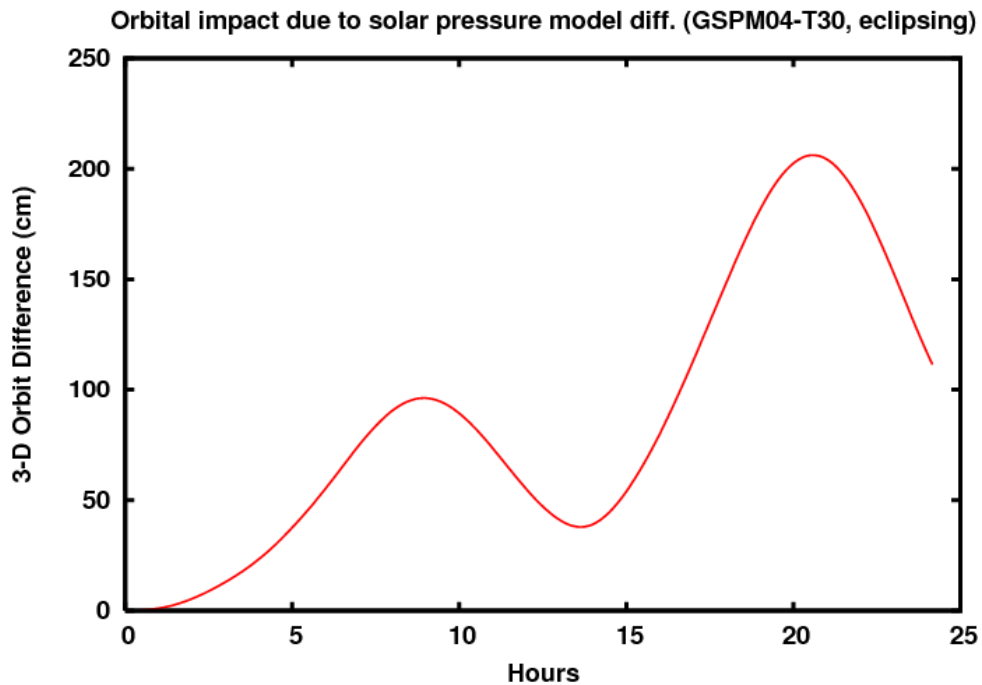


Figure 8, Eclipsing GPS57 Differences on 2008-09-01 Using GSPM04 and T30 Solar Radiation Pressure Models

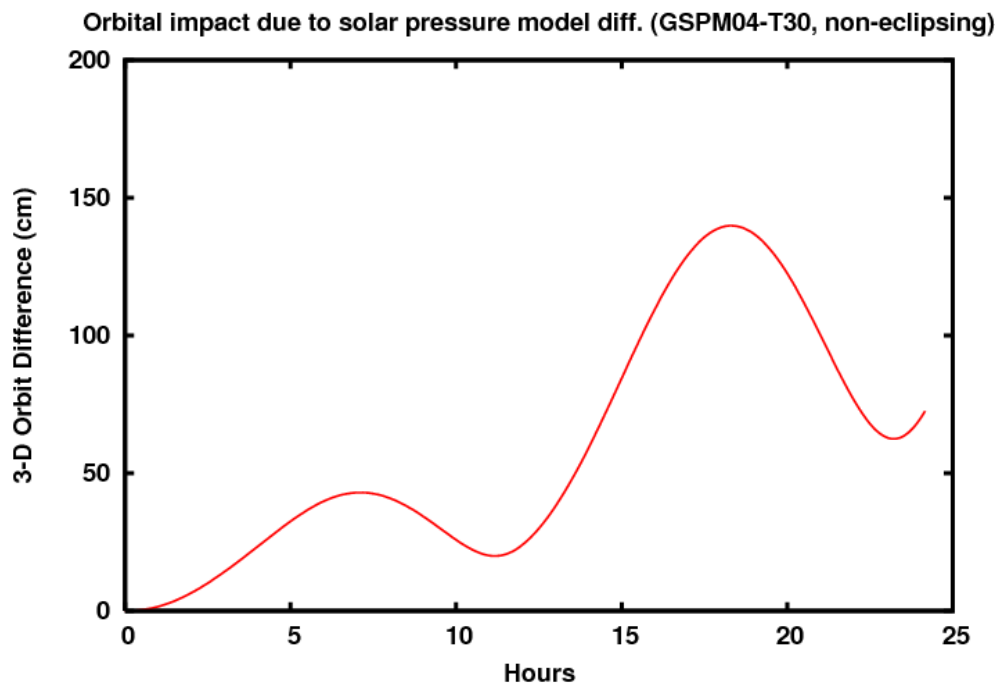


Figure 9, Non-Eclipsing GPS61 Differences on 2008-09-01 Using GSPM04 and T30 Solar Radiation Pressure Models

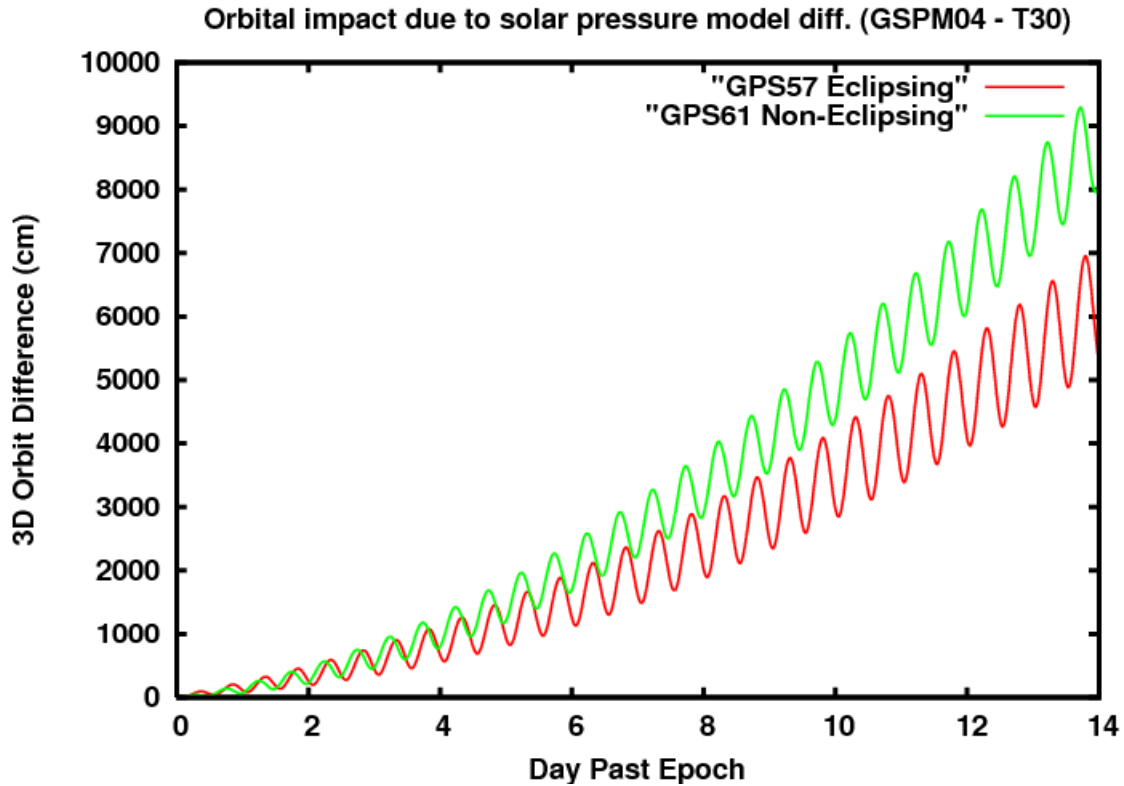


Figure 10, Differences in integrating epoch state parameters with two GPS solar pressure models over 14 days.

Earth Orientation Model Variation

We also want to investigate the impact from having some freedom in the earth orientation modeling. To represent possible differences in Earth Orientation, we used differences in in the IERS03 standards and the older IERS Tech Note 21 standards. For the 24-hour study, we used 1-day predicted polar motion and UT1 and 17-day predictions for the 14-day fit. To show the magnitude of the differences in Earth orientation, Figure 11 depicts the difference in ECI coordinates for GPS61 when the ECEF coordinates of its state are rotated to ECI with the two Earth orientation models. Radial differences are, of course, zero. Figure 12, shows the plot out to 14-days reaching a peak difference of about 4 meters.

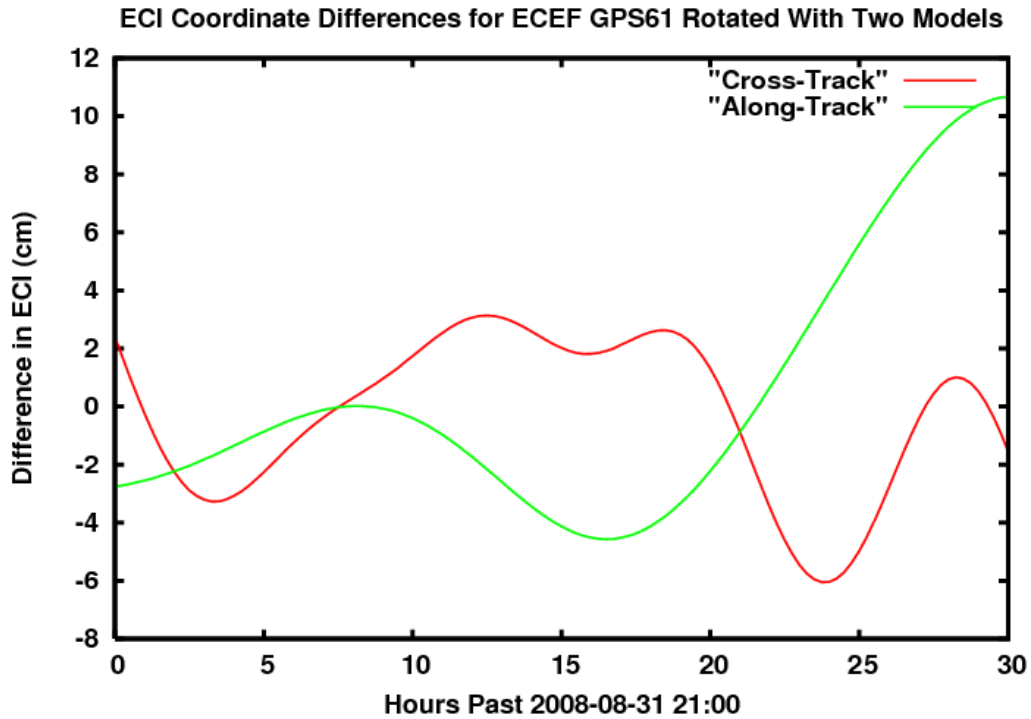


Figure 11, Differences in inertial space with two different earth orientation models. The radial difference is zero.

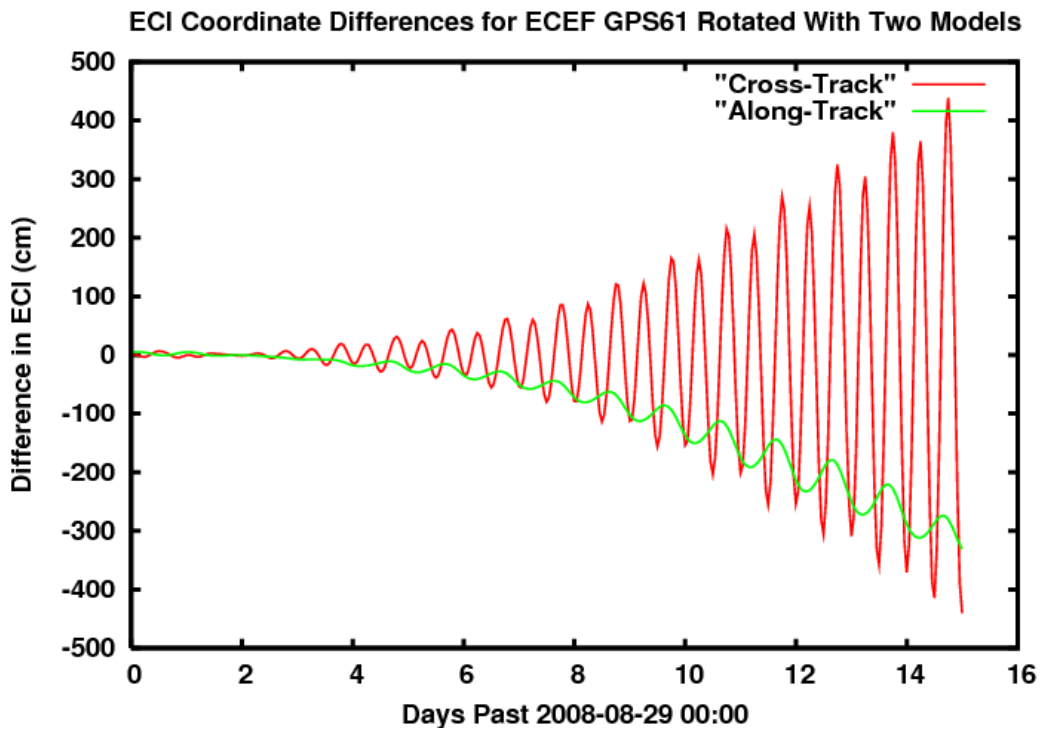


Figure 12, Differences in inertial space with two different earth orientation models. The radial difference is zero.

Results of the Least Squares Fit

For our first test we used a non-eclipsing satellite, GPS61 (SVN 61, PRN 02) for 24 hours spanning 2008-09-01 00:00 to 2008-09-02 00:00. We used the altered models detailed above in a least squares fit to these ECEF time series, estimating six epoch state parameters (position and velocity) as well as 6 model parameters. We iterated at most 4 times on the least squares solution. We then did a numerical integration of the state recovered by this fit, rotated back the position and velocity from ECI to ECEF (using the model from the fit), and compared to the reference time series (The JPL Final orbit). Using the regularly sampled time series the RMS differences in radial, cross, and along track were 1.10, 1.41, and 0.73 cm.

Since the force model differences are greater with an eclipsing satellite, we repeated the experiment with GPS57 (SVN 57, PRN 29) for this same period. We allowed for four iterations in the least squares fit. In the first iteration, the RMS fit residual was 190 cm. The subsequent iterations were all less than 2.2 cm with very small changes between iterations. Figure 13 shows the differences in the ECEF coordinates between the integrated modeled orbit and the reference orbit. RMS differences in Radial, Cross, and Along-Track are 0.96, 1.82, and 0.74 cm.

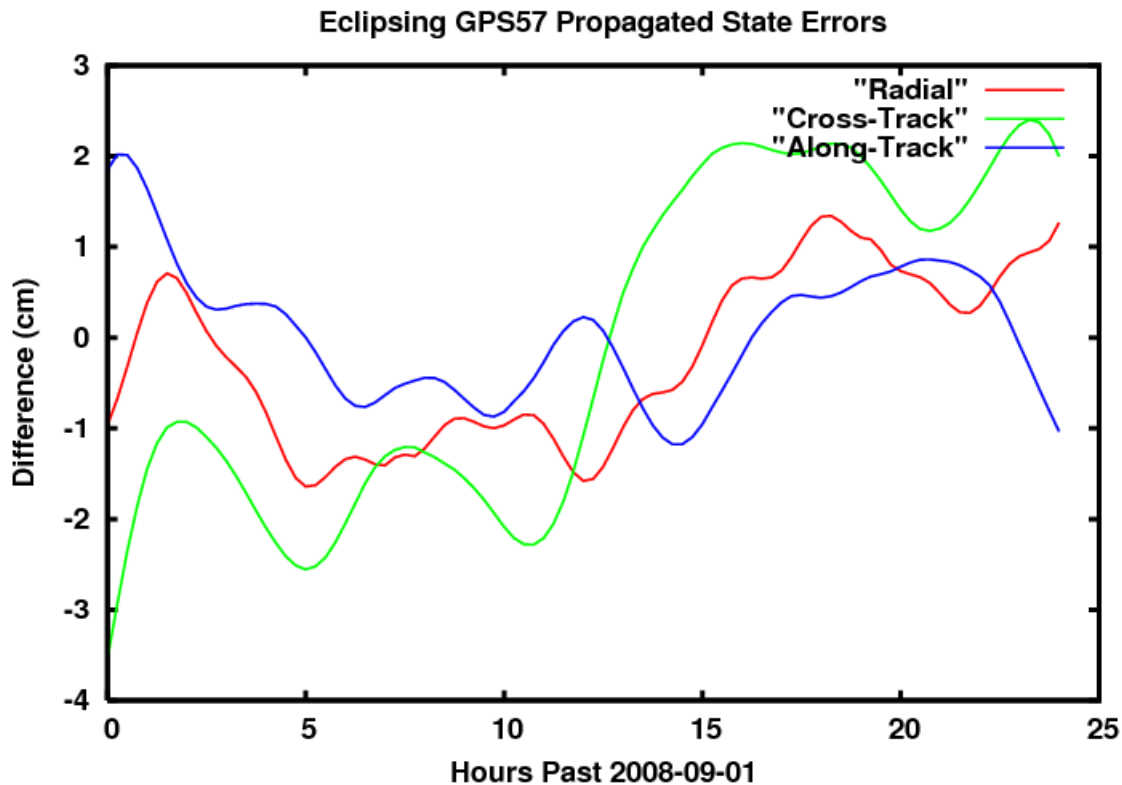


Figure 13, Differences between the truth orbit and the orbit integrated with different models after a fit.

To complete our analysis, we repeat these tests on a 14 day interval spanning 2008-08-29 00:00 to 2008-09-13 00:00 again using GPS61 and GPS57. GPS61 is in full sun during this time period. GPS57 starts eclipsing on 2008-08-31 and remains in eclipse season for the rest of the time period. Recall that we will perform our 14-day fit to the ECEF coordinates of the IGS Final with Earth Orientation degraded from truth (IERS final values and IERS03 standards) as

depicted in Fig. 12 and an older solar pressure model T30. For GPS61, the RMS difference with the IGS Final over the 14 days was 11.6, 136.8, and 76.0 cm in Radial, Cross, and Along-Track. For GPS57, the RMS was 16.6, 31.1, and 42.9 cm. Figure 14, shows the time history of these errors. The improved result for GPS57, may be due to a greater sensitivity to errors in Earth orientation in the GPS61 fit. To investigate this, we used our best model of Earth orientation (IERS finals and IERS03 standard), which of course is not possible in operations, and performed the fit again. The RMS errors decreased to 12.1, 9.8, and 16.7 cm. Finally, we also replaced the T30 solar pressure model with the GSPM-04 model and the RMS errors reduced further to 3.0, 6.2, and 6.0 cm. These results showing the sensitivity of the GPS61 14-day fit to model changes are summarized in Table 9.

Table 9, GPS61 14-day Fit Integrated Orbit Difference With Truth

Fit Model	Radial RMS(cm)	Cross-Track RMS(cm)	Along-Track RMS(cm)
T30, 17-day EO predict, Tech Note 21	11.6	136.8	76.0
T30, IERS Finals, IERS03	12.1	9.8	16.7
GSPM, IERS Finals, IERS03	3.0	6.2	6.0

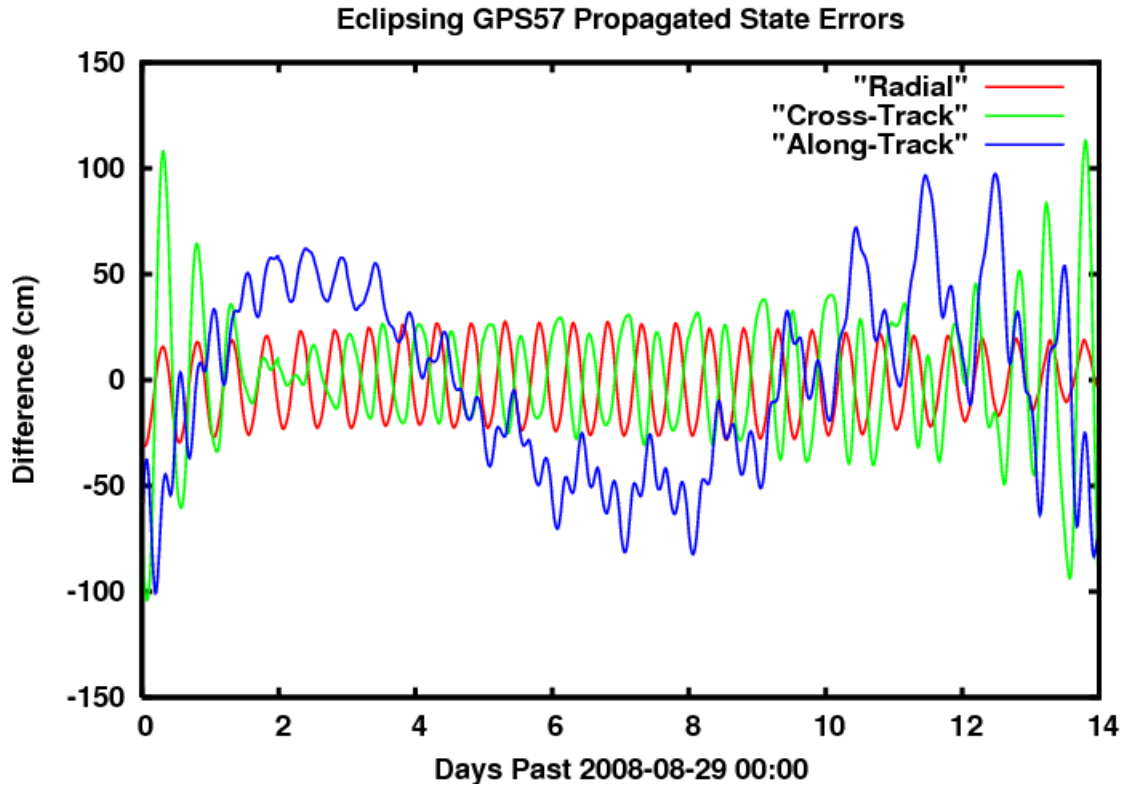


Figure 14, Errors in 14-day fit using perturbed Earth Orientation and force modeling for an eclipsing satellite.

Summary

The errors in the future GPS system are a complex combination of software, measurements, hardware, and models. For our OCX system, we have analyzed these errors and demonstrating that future users with 1-hour age of data can expect user range errors (URE) at the 15 cm level. The proposed design decouples the prediction of GPS orbits and clocks from the estimation of the zero age of data (OAOD) values. It also largely decouples the space segment software models for forces and Earth orientation from the OCX models.

Acknowledgements

Parts of the work described in this paper were performed at the Jet Propulsion Laboratory, California Institute of Technology, under contract with the National Aeronautics and Space Administration.

Jorgensen, P. S., "Navstar/Global Positioning System 18-Satellite Constellations," Global Positioning System Volume II, Institute of Navigation, pg. 1-12, 1984.

Parkinson, B. W., Vol. 1, Chapter 1, *The Global Positioning System – Theory and Application*, Senior Editors: B. W. Parkinson, J. J. Spilker, Jr.; Editors: P. Axelrad, P. Enge., AIAA, Progress in Astronautics and Aeronautics, Volume 163, pgs. 3-28, 1996.

Francisco, S. G., Vol. 1, Chapter 1, *The Global Positioning System – Theory and Application*, Senior Editors: B. W. Parkinson, J. J. Spilker, Jr.; Editors: P. Axelrad, P. Enge., AIAA, Progress in Astronautics and Aeronautics, Volume 163, pgs. 435-466, 1996.

Bertiger, W.I., Y. E. Bar-Sever, B. J. Haines, B. A. Iijima, S. M. Lichten, U. J. Lindqwister, A. J. Mannucci, R. J. Muellerschoen, T. N. Munson, A. W. Moore, L. J. Romans, B. D. Wilson, S. C. Wu, T. P. Yunck, G. Piesinger, and M. Whitehead, “A Real-Time Wide Area Differential GPS System,” *Navigation: Journal of the Institute of Navigation*, Vol. 44, No. 4, , pgs. 433-447, 1998.